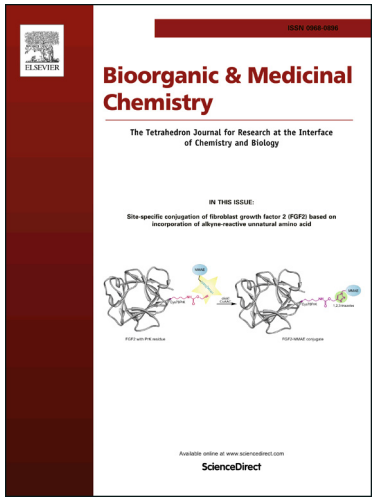

Discovery of a novel B-cell lymphoma 6 (BCL6)–corepressor interaction inhibitor by utilizing structure-based drug design

Takeshi Yasui, Takeshi Yamamoto, Nozomu Sakai, Kouhei Asano, Takafumi Takai, Yayoi Yoshitomi, Melinda Davis, Terufumi Takagi, Kotaro Sakamoto, Satoshi Sogabe, Yusuke Kamada, Weston Lane, Gyorgy Snell, Masashi Iwata, Masayuki Goto, Hiroshi Inooka, Jun-ichi Sakamoto, Yoshihisa Nakada, Yasuhiro Imaeda

PII: S0968-0896(17)31203-8
DOI: http://dx.doi.org/10.1016/j.bmc.2017.07.037
Reference: BMC 13874

To appear in: *Bioorganic & Medicinal Chemistry*

Received Date: 10 June 2017
Revised Date: 18 July 2017
Accepted Date: 19 July 2017

Please cite this article as: Yasui, T., Yamamoto, T., Sakai, N., Asano, K., Takai, T., Yoshitomi, Y., Davis, M., Takagi, T., Sakamoto, K., Sogabe, S., Kamada, Y., Lane, W., Snell, G., Iwata, M., Goto, M., Inooka, H., Sakamoto, J-i., Nakada, Y., Imaeda, Y., Discovery of a novel B-cell lymphoma 6 (BCL6)–corepressor interaction inhibitor by utilizing structure-based drug design, *Bioorganic & Medicinal Chemistry* (2017), doi: http://dx.doi.org/10.1016/j.bmc.2017.07.037

Discovery of a novel B-cell lymphoma 6 (BCL6)–corepressor interaction inhibitor by utilizing structure-based drug design

Takeshi Yasui[*, †], *Takeshi Yamamoto*[†], *Nozomu Sakai*[†], *Kouhei Asano*[†], *Takafumi Takai*[†], *Yayoi Yoshitomi*[†], *Melinda Davis*[‡], *Terufumi Takagi*[†], *Kotaro Sakamoto*[†], *Satoshi Sogabe*[†], *Yusuke Kamada*[†], *Weston Lane*[‡], *Gyorgy Snell*[‡], *Masashi Iwata*[†], *Masayuki Goto*[†], *Hiroshi Inooka*[†], *Jun-ichi Sakamoto*[†], *Yoshihisa Nakada*[†], *Yasuhiro Imaeda*[*, †]

[†]Takeda Pharmaceutical Company Limited, 26-1 Muraoka-Higashi 2-chome, Fujisawa, Kanagawa 251-8555, Japan

[‡]Takeda California Inc. 10410 Science Center Dr. San Diego CA 92121, USA

Corresponding Authors

*For T. Y.: phone, +81-466-32-4261; E-mail, takeshi.yasui@takeda.com

*For Y. I.: phone, +81-466-32-4112; E-mail, yasuhiro.imaeda@takeda.com

Abstract: B-Cell lymphoma 6 (BCL6) is a transcriptional repressor that can form complexes with corepressors via protein–protein interactions (PPIs). The complexes of BCL6 and corepressors play an important role in the formation of germinal centers (GCs), and differentiation and proliferation of lymphocytes. Therefore, BCL6–corepressor interaction inhibitors would be drug candidates for managing autoimmune diseases and cancer. Starting from high-throughput screening hits **1a** and **2a**, we identified a novel BCL6–corepressor interaction inhibitor **8c** (cell-free enzyme-linked immunosorbent assay [ELISA] IC_{50} = 0.10 μM, cell-based mammalian two-hybrid [M2H] assay IC_{50} = 0.72 μM) by utilizing structure-based drug design (SBDD) based on an X-ray crystal structure of **1a** bound to BCL6. Compound **8c** also showed a good pharmacokinetic profile, which was acceptable for both *in vitro* and *in vivo* studies.

Keywords: B cell lymphoma 6 (BCL6), protein–protein interaction (PPI), structure-based drug design (SBDD), diphenylamine

1. Introduction

B-Cell lymphoma 6 (BCL6) protein is known as a transcriptional repressor; it is composed of three domains: broad-complex, tramtrack and bric-a-brac (BTB) domain; repression domain 2 (RD2); and zinc finger (ZF) domain.[1, 2] A specific groove constructed by BCL6 BTB domain ($BCL6^{BTB}$) homodimers is involved in a protein–protein interaction (PPI) with a corepressor such as BCL6 corepressor (BCoR), silencing mediator for retinoid and thyroid receptors (SMRT), and nuclear receptor corepressor (NCoR).[3–5] BCL6 is involved in proliferation and survival of germinal center (GC) B cells, from which diffuse large B-cell lymphomas (DLBCL) originate, by recruiting the SMRT, BCoR, and NCoR corepressors to the lateral groove of the $BCL6^{BTB}$ homodimers.[6–12] Accordingly, disruption of the PPI between BCL6 and corepressors by BCL6 inhibitors may serve as a therapeutic strategy for managing autoimmune diseases and cancer.[13, 14] To date, several BCL6 inhibitors have been reported. In 2008, Evans et al. discovered rifamycin SV, a member of the ansamycin family, based on a screening of a natural product library.[15] In 2014, Leandro et al. identified a small molecular BCL6 inhibitor 79-6, which is functionally active *in vivo* and induces apoptosis of BCL6-dependent lymphoma cell lines, by a combination of computer-aided drug design and screens of small molecule libraries.[16] Further, they confirmed the binding of 79-6 to the corepressor-binding groove of $BCL6^{BTB}$ homodimers by X-ray crystallography and nuclear magnetic resonance (NMR) analysis. In 2016, the same group reported a 79-6 derivative, FX1, which showed improved potency compared to that of 79-6.[17] However, even the most active compound, FX1, among the BCL6 inhibitors reported so far has a binding affinity of only around 7 μM as a K_D value. In general, development of small molecular PPI inhibitors is relatively difficult mainly because of following reasons[18–20]: (1) Contact surfaces involved in PPIs are relatively large compared to those of conventional targets such as enzymes or G-protein-coupled receptors (GPCRs); and (2) regions of residues that contribute to high-

affinity binding, called hotspots, are generally small on the protein–protein interface. Accordingly, PPI inhibitors tend to have low ligand efficiency and high molecular weights.

Very recently, we identified a BCL6 inhibiting tridecapeptide, F1324 (Ac-LWYTDIRMSWRVP-OH), which binds to the corepressor-binding groove of the $BCL6^{BTB}$ homodimers and inhibits PPI between $BCL6^{BTB}$ and BCoR with strong K_D and IC_{50} values (0.57 nM and 1 nM, respectively).[21, 22] Interestingly, an evaluation of truncated tetrapeptides of F1324 revealed that the C-terminus tetrapeptide region of F1324 (WRVP-OH) plays an important role in potentiation. In addition, according to the X-ray co-crystal structure of 79-6 with $BCL6^{BTB}$, the binding site of 79-6 is the same as the C-terminus tetrapeptide-binding region.[16] On the basis of these findings, it was suggested that the corepressor-binding groove of the $BCL6^{BTB}$ homodimers could have a hotspot for small molecular inhibitors to bind with high affinity. Herein, we report the identification of diphenylamine derivatives as BCL6 inhibitors by high-throughput screening (HTS) and their subsequent structure-based optimization into a cellular potent BCL6 inhibitor with a good pharmacokinetic profile.

2. Chemistry

Synthesis of diphenylamine derivatives **1b–h** is shown in Scheme 1. S_NAr displacement reaction of the commercially available aryl fluorides **10b–f** with 5-amino-2-benzimidazolinone **9** gave the corresponding diphenylamine derivatives **1b–f**. Carboxylic acid **1g** was prepared from ester **1f** by hydrolysis. Subsequent amidation of **1g** with $HOBt{\cdot}NH_3$ afforded carboxamide **1h**. Hereinafter, the left-hand side aryl group and the right-hand side aryl group of the diphenylamine compounds are referred to as "ring A" and "ring B," respectively, as described in Scheme 1.

Scheme 1. Synthesis of **1b–h**[a]

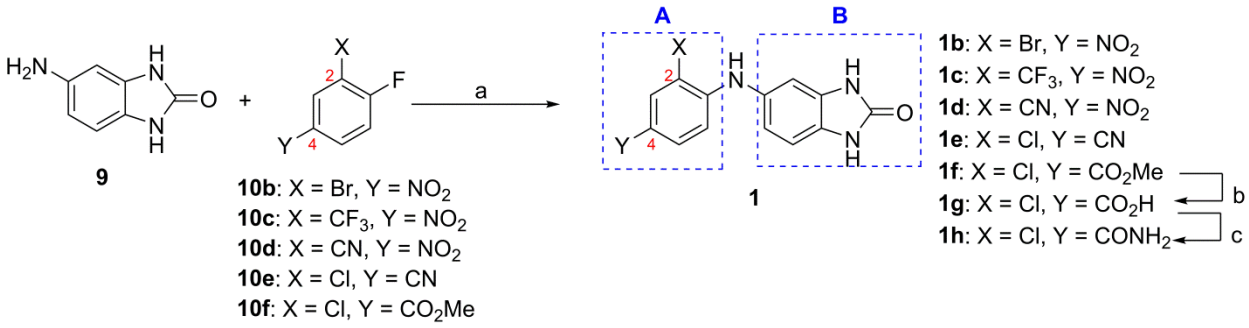

[a] Reagents and conditions: (a) TEA or DIPEA, DMSO, rt–160 °C, 2 h–3 d, 1–80%; (b) 1 M NaOH, MeOH, THF, 50 °C, 3 h, 57%; (c) HOBt·NH_3, EDC, DMF, rt, 4 d, 70%.

Introduction of substituents to the 5-position of ring A of **1a** was achieved in two steps (Scheme 2). Intermediates **13a–d** were obtained by the S_NAr displacement reaction of aryl fluoride **11** with the corresponding commercially available amines **12a–d**. Ether **13e** was prepared from **11** and 4-hydroxytetrahydropyran **12e** in the presence of sodium hydride. Treatment of **13a** and **13b** with aniline **9** under microwave irradiation provided alcohol **3** and ester **4**, respectively. Subsequent hydrolysis of **4** provided carboxylic acid **5**. Intermediates **13c–e** were employed for syntheses of **6**, **7**, and **8a** via a palladium (Pd)-mediated cross-coupling reaction, Buchwald-Hartwig amination, with aniline **9**.

Scheme 2. Synthesis of **3–8a**[a]

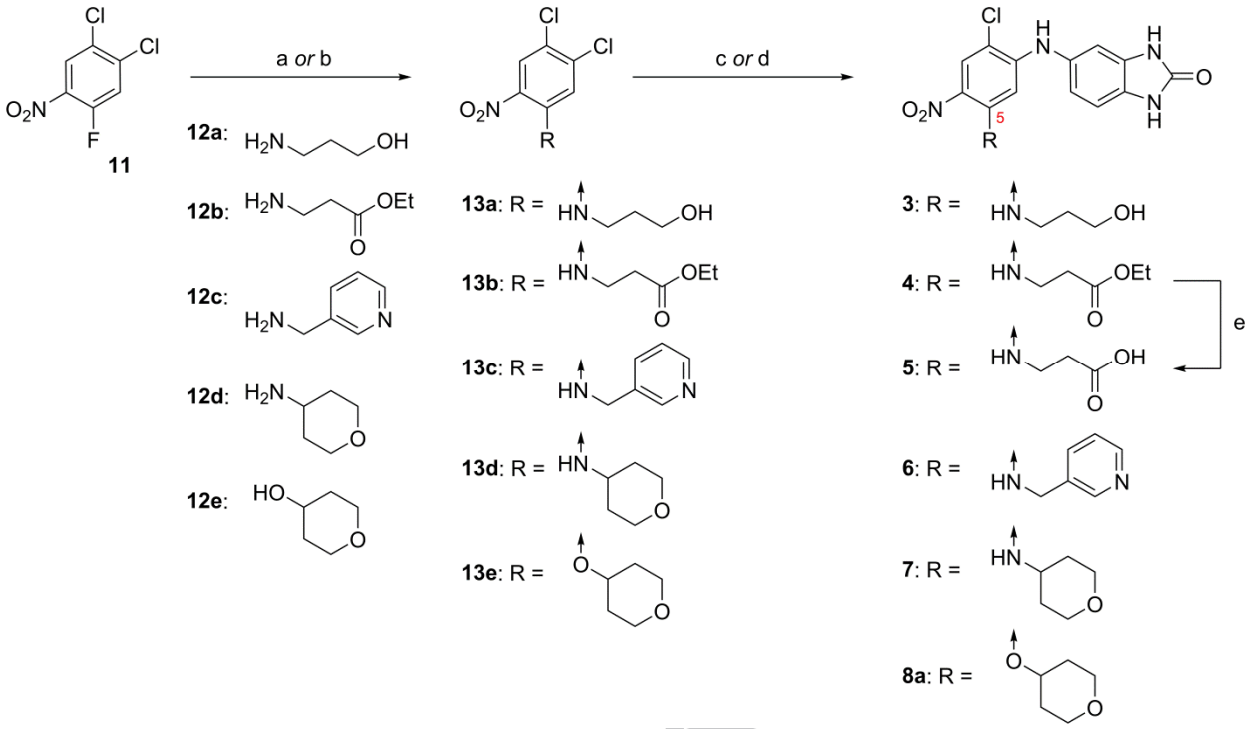

[a] Reagents and conditions: (a) **12a–d**, TEA or DIPEA, DMA, or DMSO, rt, 3–16 h, 85–89%; (b) **12e**, NaH, DMF, 0 °C, 20 min, 58%; (c) **9**, DIPEA, DMA, or NMP, MW, 150–200 °C, 2–3 h, 5–31%; (d) **9**, $Pd_2(dba)_3$, BINAP, Cs_2CO_3, DME, 100 °C, 4–16 h, 5–47%; (e) 2 M NaOH, THF, MeOH, rt, 16 h, 47%.

Installation of an oxindole scaffold as ring B by the Buchwald-Hartwig amination of **13e** with 5-aminoindolin-2-one gave compound **8b** (Scheme 3). In the same manner, 3,4-dihydroquinolinones **8c** were prepared from **13e** with 6-amino-3,4-dihydroquinoline-2(1*H*)-one.

Scheme 3. Synthesis of **8b**–**c**[a]

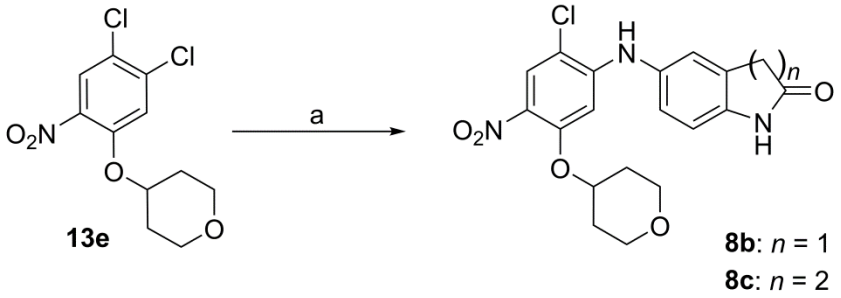

[a] Reagents and conditions: (a) 5-aminoindolin-2-one or 6-amino-3,4-dihydroquinolin-2(1*H*)-one, $Pd_2(dba)_3$, BINAP, Cs_2CO_3, DME, 100 °C, 4 h, 17–56%.

3. Results and discussion

3. 1. PPI inhibitory activities

The synthesized compounds were evaluated by an enzyme-linked immunosorbent assay (ELISA) as the primary cell-free assay to determine the PPI inhibitory activities (IC_{50}) between $BCL6^{BTB}$ and BCoR. HTS of around 130,000 compounds using the ELISA monitoring the interaction between the $BCL6^{BTB}$ and the BCoR peptide provided diphenylamine derivatives **1a** and **2a** as chemical starting points for $BCL6^{BTB}$-BCoR PPI inhibition (Fig. 1). The hit compounds **1a** and **2a** displayed more potent inhibitory activities (IC_{50} = 4.5 and 14 μM, respectively) than that of the reported compound 79-6 (IC_{50} = 200 μM).[16] The IC_{50} value of 79-6 in our ELISA system was comparable to the reported data (IC_{50} = 212 μM). The binding of **1a** or **2a** to BCL6 protein was confirmed by surface plasmon resonance (SPR) and their affinities (K_D values) against $BCL6^{BTB}$ were similar to their IC_{50} values (**1a**, K_D = 5.0 μM; **2a**, K_D = 24 μM). The reported K_D value of FX1 is 7 μM determined by microscale thermophoresis.[17]

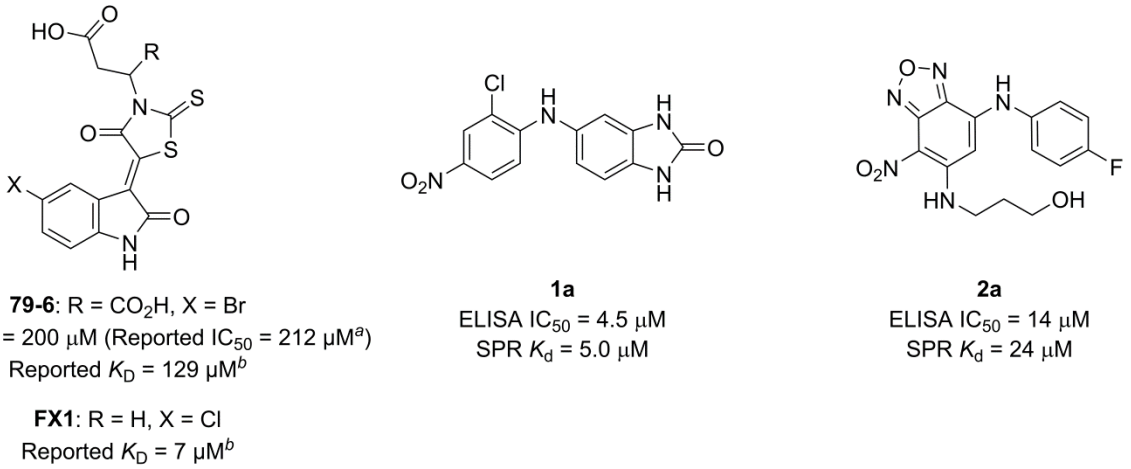

Fig 1. Known BCL6 inhibitors 79-6 and FX1, and hit compounds **1a** and **2a** from HTS. [a] Displacement of a SMRT-BBD peptide from $BCL6^{BTB}$ corepressor complex was measured by a fluorescence polarization competitive binding assay.[16] [b] Determined by microscale thermophoresis.[17]

With the aim of improving the PPI inhibitory activity and exploring the structure-activity relationship (SAR), effects of substituents at the 2- and 4-positions of ring A of **1a** were investigated. The results are summarized in Table 1. Replacement of the chlorine atom of **1a** with a bromine atom (**1b**) or trifluoromethyl group (**1c**) led to a reduction of the inhibitory activity (IC_{50} = 83 and > 300 μM, respectively). On the other hand, the cyano derivative **1d** showed potency similar to that of **1a** (IC_{50} = 4.3 μM). Regarding the replacement of the nitro group at the 4-position of **1a**, the cyanide (**1e**), ester (**1f**), carboxylic acid (**1g**), and carboxamide (**1h**) derivatives resulted in decreased inhibitory activities.

Table 1. Effects of the 2-, 4-substituents of ring A on cell-free PPI inhibition

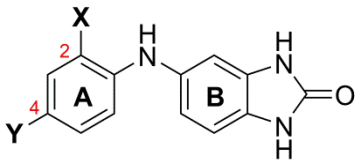

Compounds	X	Y	ELISA IC_{50} (μM)[a, b]
1a	Cl	NO_2	4.5 (3.5–5.7)
1b	Br	NO_2	83 (22–310)
1c	CF_3	NO_2	>300
1d	CN	NO_2	4.3 (3.9–4.9)
1e	Cl	CN	110 (23–490)
1f	Cl	CO_2Me	8.6 (4.7–16)
1g	Cl	CO_2H	62 (50–75)
1h	Cl	$CONH_2$	43 (37–51)

[a] Inhibition of BCL6-corepressor (BCoR) interaction was measured. [b] 95% confidence intervals are shown in parentheses.

3. 2. X-ray crystal structure

To elucidate and further investigate the binding mode of **1a** to $BCL6^{BTB}$, an X-ray crystallographic analysis was conducted. It revealed that **1a** binds to a part of the corepressor-binding groove, which is the same site as that of 79-6 in the crystal structure of a $BCL6^{BTB}$/79-6 complex[16] and/or tetrapeptide Ac-WRVP-OH in the crystal structure of a $BCL6^{BTB}$/F1324(10–13) complex[21] (Fig. 2). In the crystal structure of **1a** bound to $BCL6^{BTB}$, the ring A moiety is positioned in a hydrophobic pocket composed of side chains of Tyr58, Asn21, Arg24, and Arg28 (Fig. 2a). A hydrogen bond between the NH group of the diphenylamino moiety and the carbonyl group of the backbone of Met51 is observed (Fig. 2b). The chlorine atom at the 2-position of **1a** fully occupies the relatively small hydrophobic pocket surrounded by Met51, Leu25, and Ala52, as shown in Fig. 2a. This binding mode information is consistent with the fact

that the relatively large substituents, such as the bromine atom and trifluoromethyl group, were not tolerated as substituents at the 2-position of **1a**.

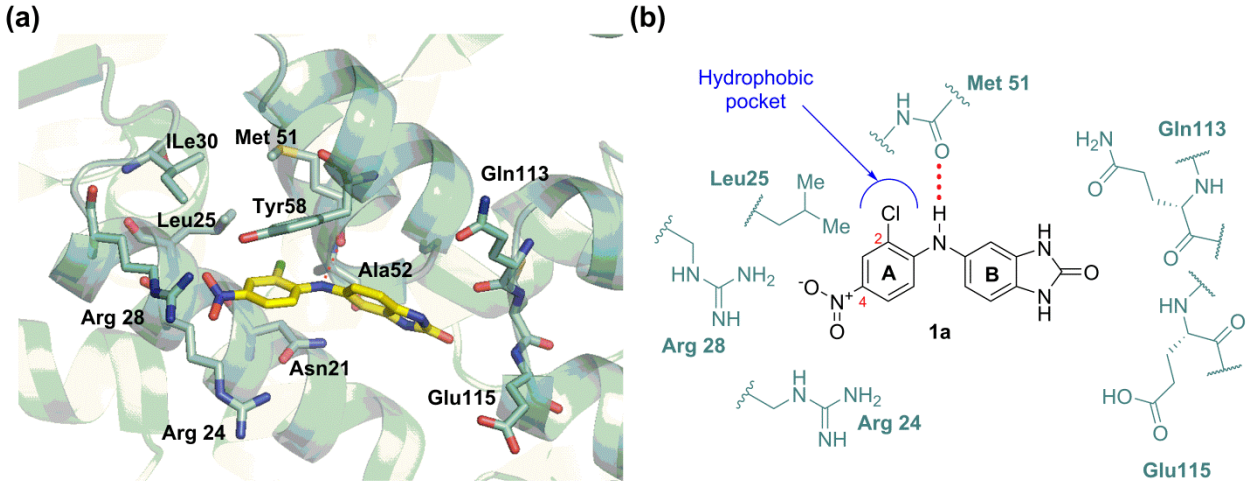

Fig. 2. X-ray crystal structure of **1a** with BCL6 (PDB code: 5X9O). (a) Amino acid residues of BCL6 and **1a** are shown in light green and yellow, respectively. (b) Schematic diagram of the ligand binding site.

3. 3. Docking simulation

Regarding the benzoxadiazole derivative **2a** identified from HTS, removal of the hydroxypropyl group (**2b**) resulted in a 5-fold decrease in potency (IC_{50} = 69 μM, Fig. 3a). This data suggested that the hydroxypropyl group formed an interaction with some residues on $BCL6^{BTB}$, and contributed to the improvement of the potency. To estimate the binding mode, a docking model of **2a** with BCL6 was constructed by MOE using the BCL6/**1a** complex structure.[23] The docked pose of **2a** overlaid well with the binding mode of the **1a**-bound BCL6

crystal structure (Fig. 3b). In this docking model, the alcohol moiety of the hydroxypropyl group of **2a** was located in the vicinity of Arg28, and the interaction between the alcohol moiety and the guanidyl side chain of Arg28 was indicated. Based on this docking study, the hydroxypropylamino group was introduced into the 5-position of ring A of **1a**. As a result, the hybridized compound **3** showed a 20-fold improvement in BCL6^{BTB}–BCoR PPI inhibitory potency (IC_{50} = 0.24 μM) as compared with that of **1a**.

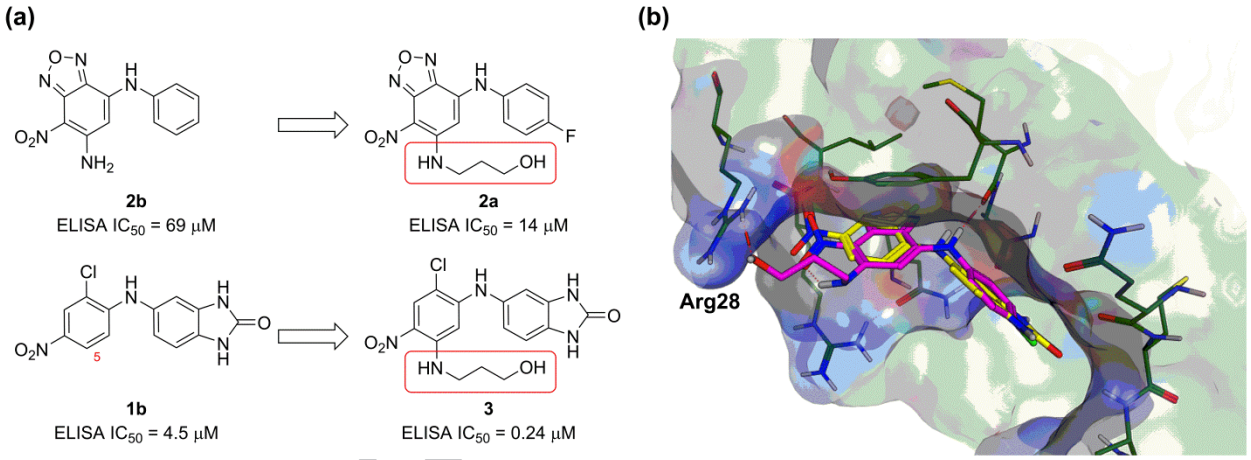

Fig. 3. Presumed effect of hydroxypropylamino group of **2a** by docking study. (a) Introduction of the hydroxypropylamino group led to improvement of the potency. (b) Superposition of BCL6-bound **1a** (yellow) and the docking structure of **2a** (magenta) constructed by MOE. A hydrogen bonding between the hydroxy group of **2a** and the guanidyl side chain of Arg28 is suggested. Some amino acid residues were omitted for clarification.

3. 4. Physicochemical properties

Although inhibitory activity was improved, compound **3** displayed insufficient aqueous solubility (0.09 μg/mL) and parallel artificial membrane permeability assay (PAMPA) permeability (undetected) under neutral conditions (at pH 6.8 for aqueous solubility and 7.4 for PAMPA). To improve these physicochemical properties that could affect its cellular activity, conversion of the substituent at the 5-position of ring A was explored, and the results are summarized in Table 2. Ester **4** exhibited improved PAMPA permeability (151 nm/s) with good PPI inhibitory activity (IC_{50} = 0.43 μM), although its aqueous solubility remained low (0.42 μg/mL). On the other hand, carboxylic acid **5** showed high aqueous solubility (> 72 μg/mL) while its PAMPA permeability was poor. Introduction of a 3-pyridylmethylamino group (**6**) or 4-tetrahydropyranylamino group (**7**) at the 5-position resulted in enhancement of the potencies (IC_{50} = 0.15 and 0.13 μM, respectively), although their aqueous solubilities were still insufficient (< 0.23 and 0.61 μg/mL, respectively). Interestingly, the 4-tetrahydropyranyloxy derivative **8a** exhibited significantly improved aqueous solubility (18 μg/mL) while maintaining high potency (IC_{50} = 0.22 μM) and moderate PAMPA permeability (45 nm/s). The significantly improved aqueous solubility of **8a** might be attributed to its more flexible conformation through disruption of the planar conformation due to its intramolecular hydrogen bond between the oxygen atom of the nitro group and the NH group of the 4-tetrahydropyranylamino moiety of **7a**.[24, 25]

Table 2. Effects of the 5-substituent of ring A on cell-free PPI inhibition, solubility, and membrane permeability

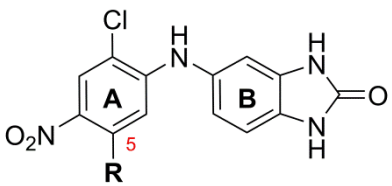

Compound	**R**	ELISA IC_{50} (μM)[a, b]	Aqueous solubility (μg/mL)[c]	PAMPA (nm/s)[d]
3	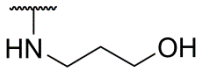	0.24 (0.18–0.33)	0.09	undetected
4	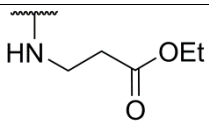	0.43 (0.37–0.50)	0.42	151
5	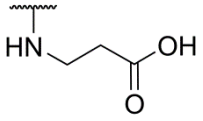	0.13 (0.10–0.15)	>72	undetected
6	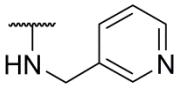	0.15 (0.12–0.19)	<0.23	147
7	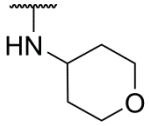	0.13 (0.11–0.15)	0.61	101
8a	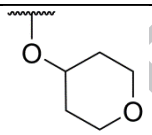	0.22 (0.18–0.27)	18	45

[a] Inhibition of BCL6-corepressor (BCoR) interaction was measured. [b] 95% confidence intervals are shown in parentheses. [c] Measured at pH 6.8. [d] Measured at pH 7.4.

Compounds **3–8a**, whose PPI inhibitory activities were improved by introducing side chains with a hydrogen bond acceptor (HBA) into **1a**, were crystallized in complex with BCL6 to clarify binding modes. An X-ray crystal structure of carboxylic acid **5** bound to BCL6 was obtained. It elucidated that **5** binds to the same site as **1a** in the same manner (Fig. 4). However,

the electron density map showed that the carboxylate moiety of **5** is exposed to solvent and mostly disordered (data not shown). No clear interactions were observed between the carboxylate moiety and the guanidyl side chain of Arg28, and the effect of the carboxylate moiety for the improved potency remains unclear because no specific structural features are observed.

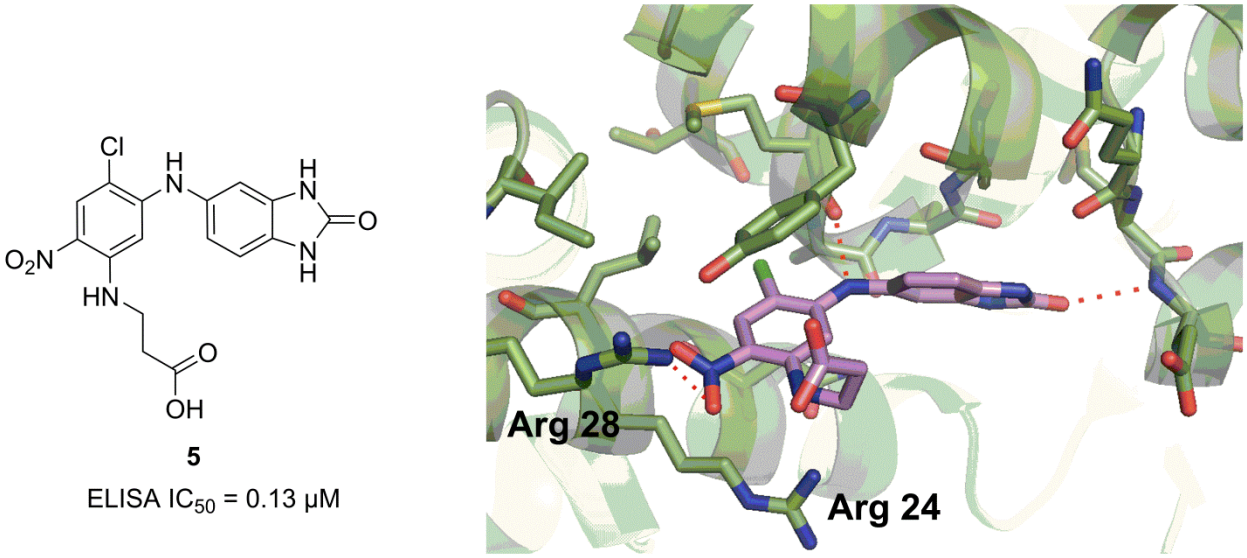

Fig. 4. X-ray crystal structure of **5** bound to BCL6 (PDB code: 5X9P)

Our next efforts were focused on modification of ring B for further improvement of membrane permeability. The benzimidazolone scaffold (**8a**) with two hydrogen bond donors (HBDs) was considered to be one of the reasons for the low PAMPA permeability. Therefore, we synthesized oxindole **8b** and tetrahydroquinolinone **8c** to improve PAMPA permeability while maintaining potency. As expected, the PAMPA permeabilities of **8b** and **8c** (288 and 206 nm/s, respectively) were dramatically improved compared with that of **8a** (45 nm/s). The

potency and aqueous solubility of **8b** (IC_{50} = 0.13 μM, aqueous solubility = 12 μg/mL) and **8c** (IC_{50} = 0.10 μM, aqueous solubility = 12 μg/mL) were comparable to those of **8a** (IC_{50} = 0.22 μM, aqueous solubility = 18 μg/mL). In addition, **8b** and **8c** did not exhibit significant cytotoxicity even at 30 μM (Table 3).

Table 3. *In vitro* profiles of diphenylamine derivatives having modified ring B

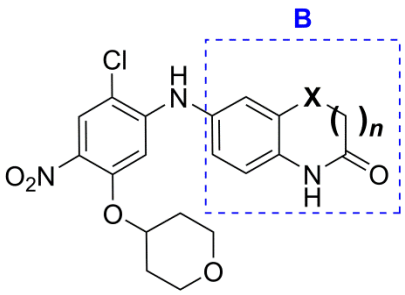

	X = NH, *n* = 0	X = CH_2, *n* = 0	X = CH_2, *n* = 1
Compound	**8a**	**8b**	**8c**
ELISA IC_{50} (μM)[a, b]	0.22 (0.18–0.27)	0.13 (0.12–0.15)	0.10 (0.091–0.12)
Aqueous solubility (μg/mL)[c]	18	12	12
PAMPA (nm/s)[d]	45	288	206
Cytotoxicity (ATP, % at 30 μM)	100	99	83

[a] Inhibition of BCL6-corepressor (BCoR) interaction was measured. [b] 95% confidence intervals are shown in parentheses. [c] Measured at pH 6.8. [d] Measured at pH 7.4.

3. 5. Cell-based M2H assay

Compounds **8b** and **8c**, having improved physicochemical properties, were further evaluated in a cell-based assay using a mammalian two-hybrid (M2H) system (Table 4). Cellular PPI inhibition between $BCL6^{BTB}$ and BCoR by **8b** was observed with an IC_{50} value of 1.2 μM. Compound **8c** also exhibited good cellular PPI inhibitory activity in the submicromolar range (M2H IC_{50} = 0.72 μM). Although the cell-free PPI inhibitory activity of compound **3** was comparable to those of **8b** and **8c**, no cellular activity was observed even at 100 μM of **3**, indicating that its physicochemical properties were inadequate.

Table 4. Cell-based PPI inhibition of diphenylamine derivatives using M2H method

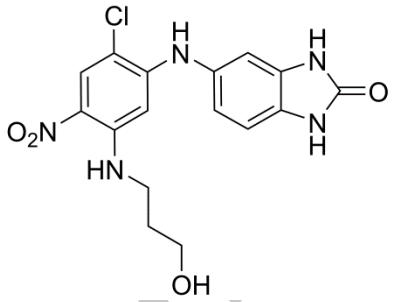

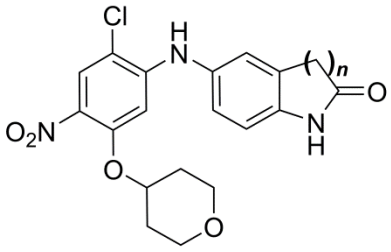

Compound	**3**	**8b** (n = 1)	**8c** (n = 2)
M2H IC_{50} (μM)[a]	>100	1.2	0.72

[a] Inhibition of BCL6-corepressor (BCoR) interaction was measured.

3. 6. PK profiles

The pharmacokinetic profile of compound **8c** was evaluated by a mouse cassette-dosing study (0.1 mg/kg iv; 1 mg/kg po). As summarized in Fig. 5, compound **8c** exhibited a good

pharmacokinetic profile (MRT = 3.3 h, AUC = 1.27 μg•h/mL, F = 79.9%). These data indicate that compound **8c** could be utilized as a tool compound for *in vitro* and *in vivo* biological studies.

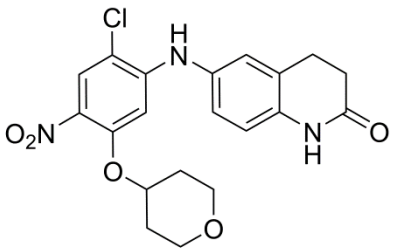

8c

C_{max}	233 ng/mL
T_{max}	2.0 h
AUC	1.27 μg•h/mL
MRT	3.3 h
F	79.9%
Cl_{total}	630 mL/h•kg
VD_{ss}	1505 mL/kg

Fig. 5. Pharmacokinetic parameters for **8c** by mouse cassette-dosing (0.1 mg/kg iv; 1 mg/kg po). C_{max} = maximal plasma concentration reached after oral administration. T_{max} = time to reach the maximal plasma concentration after oral administration. MRT = mean residence time after oral administration. F = oral bioavailability. AUC = exposure (total area under the plasma concentration–time curve) after oral administration. Cl_{total} = total clearance. VDss = volume of distribution.

4. Conclusion

Novel BCL6^{BTB}-BCoR PPI inhibitors were identified by a structure-based drug design (SBDD) approach starting from the HTS hit compounds **1a** and **2a**. On the basis of the superposition of the X-ray crystal structure of **1a** bound to BCL6 and the docking model of **2a**, we designed diphenylamine **3** by introducing a hydroxypropylamino group, and it showed the significantly improved PPI inhibitory activity compared to that of **1a**. Further exploration of the substituents on rings A and B of **3** led to the identification of oxindole **8b** and

tetrahydroquinolinone **8c** with approximately 40-fold greater PPI inhibitory activities than that of **1a**. They also exhibited sufficient membrane permeabilities and aqueous solubilities to give measurable activity in the M2H assay. Evaluation of **8b** and **8c** by the M2H assay demonstrated good cellular PPI inhibitory activities with IC_{50} values of 1.2 μM and 0.72 μM, respectively. In addition, the good pharmacokinetic profile of **8c** in mice indicated that **8c** could be a suitable chemical probe as a BCL6 inhibitor for both *in vivo* and *in vitro* experiments. Although PPI inhibitors tend to be larger molecules (MW ≥ 500) than enzyme inhibitors in general,[26] the molecular weights of our compounds remained around 400. We believe this research is a good example of how an SBDD approach can work efficiently against PPI targets.

5. Experimental section

5. 1. Chemistry

Melting points were determined on a Büchi melting point apparatus B-545 and were uncorrected. Proton nuclear magnetic resonance (^{1}H NMR) spectra were recorded on Bruker AVANCE-300 (300 MHz) instruments in $CDCl_3$ or DMSO-d_6 solution. Chemical shifts are given in parts per million (ppm) with tetramethylsilane as an internal standard. Abbreviations are used as follows: s = singlet, d = doublet, t = triplet, q = quartet, quin = quintet, m = multiplet, dd = doublet of doublets, dt = doublet of triplets, brs = broad singlet. Coupling constants (*J* values) are given in hertz (Hz). Elemental analyses were carried out by Elemental Microanalysis Team in Medicinal Chemistry Research Laboratories and were within 0.4% of the theoretical values unless otherwise noted. Low-resolution mass spectra (MS) were acquired using an Agilent LC/MS system (Agilent1200SL/Agilent6130MS or Agilent1200SL/Agilent1956MS or

Agilent1200SL/Agilent6110MS), Shimadzu UFLC/MS (Prominence UFLC high pressure gradient system/LCMS-2020) operating in electron spray ionization mode (ESI+). The column used was an L-column 2 ODS (3.0 x 50 mm I.D., 3 μm, CERI, Japan) with a temperature of 40 °C and a flow rate of 1.2 or 1.5 ml/min. Condition 1: Mobile phases A and B under an acidic condition were 0.05% TFA in water and 0.05% TFA in MeCN, respectively. The ratio of mobile phase B was increased linearly from 5% to 90% over 0.9 min, 90% over the next 1.1 min. Condition 2: Mobile phases A and B under a neutral condition were a mixture of 5 mmol/L $AcONH_4$ and MeCN (9:1, v/v) and a mixture of 5 mmol/L $AcONH_4$ and MeCN (1:9, v/v), respectively. The ratio of mobile phase B was increased linearly from 5% to 90% over 0.9 min, 90% over the next 1.1 min.

The purities of all compounds tested in biological systems were assessed as being > 95% using elemental analysis or analytical HPLC. Purity data were collected by HPLC with NQAD (Nano Quality Analyte Detector) or Corona CAD (Charged Aerosol Detector). The column was an L-column 2 ODS (30 x 2.1 mm I.D., CERI, Japan) or a Capcell Pak C18AQ (50 mm x 3.0 mm I.D., Shiseido, Japan) with a temperature of 50 °C and a flow rate of 0.5 ml/min. Mobile phases A and B under a neutral condition were a mixture of 50 mmol/L ammonium acetate, water and acetonitrile (1:8:1, v/v/v) and a mixture of 50 mmol/L ammonium acetate and MeCN (1:9, v/v), respectively. The ratio of mobile phase B was increased linearly from 5% to 95% over 3 min, 95% over the next 1 min. Reagents and solvents were obtained from commercial sources and used without further purification.

Reaction progress was determined by thin layer chromatography (TLC) analysis on Merck Kieselgel 60 F254 plates or Fuji Silysia NH plates. Chromatographic purification was carried out on silica gel columns ((Merck Kieselgel 60, 70–230 mesh or 230–400 mesh, Merck),

(Chromatorex NH-DM 1020, 100–200 mesh, Fuji Silysia Chemical, Ltd.) or (Inject column and Universal column, YAMAZEN Co.)) or on Purif-Pack (Si or NH, Shoko Scientific Co., Ltd.). Preparative HPLC were acquired using a Gilson Preparative HPLC System (GX-D) with UV detector (220 and 254 nm). The column used was a Symmetrix ODS-R (150 x 30 mm I.D., 5 μm, Boston Analytics, Inc. China) and a flow rate of 25 ml/min. Condition 1: Mobile phases A and B under an acidic condition were 0.225% formic acid in water and MeCN, respectively. Condition 2: Mobile phases A and B under a basic condition were 0.05% ammonium hydroxide in water and MeCN, respectively. The ratio of mobile phase B was increased linearly over between 8 and 15 min. All commercially available solvents and reagents were used without further purification. Yields were not optimized. The following abbreviations are used. $CDCl_3$, deuterated chloroform; DMA, *N*,*N*'-dimethylacetamide; DME, 1,2-dimethoxyethane; DMF, *N*,*N*-dimethylformamide; DMSO, dimethyl sulfoxide; DMSO-d_6, dimethyl sulfoxide-d_6; DIPEA, *N*,*N*-diisopropylethylamine; EDC, 1-[3-(dimethylamino)propyl]-3-ethylcarbodiimide; EtOAc, ethyl acetate; EtOH, ethanol; HOBt·NH_3, 1-hydroxybenzotriazole ammonium salt; IPE, diisopropyl ether; MeCN, acetonitrile; MeOH, methanol; NMP, 1-methyl-2-pyrrolidone; $Pd_2(dba)_3$, Tris(dibenzylideneacetone)dipalladium(0); BINAP, racemic-2,2'-bis(diphenylphosphino)-1,1'-binaphthyl; TEA, triethylamine; TFA, trifluoroacetic acid; THF, tetrahydrofuran.

5-((2-Bromo-4-nitrophenyl)amino)-1H-benzo[d]imidazol-2(3H)-one (***1b***)

To a solution of compound **9** (149 mg, 1.0 mmol) and TEA (0.21 mL, 1.5 mmol) in DMSO (4 mL) was added compound **10b** (242 mg, 1.1 mmol) at rt. The mixture was stirred at rt for 3 d and at 50 °C for 1 d. The reaction mixture was cooled to rt and diluted with MeCN (4 mL) and water. The precipitated solid was collected by filtration, washed with MeCN–water (1:1) and

water, and dried to give compound **1b** (145 mg, 0.42 mmol, 42%) as an orange solid. ^{1}H NMR (DMSO-d_6) 6.79 (1H, d, J = 9.3 Hz), 6.83–6.89 (2H, m), 6.95–7.00 (1H, m), 8.00 (1H, dd, J = 9.3, 2.6 Hz), 8.35 (1H, d, J = 2.6 Hz), 8.38 (1H, brs), 10.70 (2H, brs). MS m/z 351 $(M+H)^+$. Mp 299–301 ºC. Anal. Calcd for $C_{13}H_9BrN_4O_3 \cdot 2.7H_2O$: C, 39.25; H, 3.65; N, 14.08. Found: C, 39.08; H, 3.46; N, 14.02.

*5-((4-Nitro-2-(trifluoromethyl)phenyl)amino)-1H-benzo[d]imidazol-2(3H)-one (**1c**)*

To a solution of compound **9** (149 mg, 1.0 mmol) and TEA (0.21 mL, 1.5 mmol) in DMSO (4 mL) was added compound **10c** (0.15 mL, 1.1 mmol) at rt. The mixture was stirred at rt for 3 d and diluted with EtOH (2 mL) and water (6 mL). The precipitated solid was collected by filtration, washed with MeCN–water (1:1), water and MeCN, and dried to give compound **1c** (157 mg, 0.46 mmol, 46%) as a yellow solid. ^{1}H NMR (DMSO-d_6) 6.78–6.89 (3H, m), 6.99 (1H, d, J = 8.1 Hz), 8.15 (1H, dd, J = 9.4, 2.6 Hz), 8.30 (1H, d, J = 2.6 Hz), 8.65 (1H, s), 10.74 (2H, s). MS m/z 339 $(M+H)^+$. Mp 279–281 ºC. Anal. Calcd for $C_{14}H_9F_3N_4O_3 \cdot 0.25H_2O$: C, 49.06; H, 2.79; N, 16.35. Found: C, 49.15; H, 2.67; N, 16.18.

*5-Nitro-2-((2-oxo-2,3-dihydro-1H-benzo[d]imidazol-5-yl)amino)benzonitrile (**1d**)*

To a solution of compound **9** (149 mg, 1.0 mmol) and TEA (0.21 mL, 7.5 mmol) in DMSO (4 mL) was added compound **10d** (183 mg, 1.1 mmol) at rt. The mixture was stirred at rt for 3 d, diluted with EtOH (2 mL) and water (4 mL). The precipitated solid was collected by filtration and washed with MeCN–water (1:1). The solid was suspended in MeCN, collected by filtration, washed with MeCN, and dried to give compound **1d** (237 mg, 0.80 mmol, 80%) as an orange solid. ^{1}H NMR (DMSO-d_6) 6.85–6.99 (4H, m), 8.15 (1H, dd, J = 9.5, 2.7 Hz), 8.51 (1H, d, J =

2.7 Hz), 9.36 (1H, s), 10.72 (2H, s). MS *m/z* 296 $(M+H)^+$. Mp 342–344 ºC. Anal. Calcd for $C_{14}H_9N_5O_3 \cdot 0.4H_2O$: C, 55.59; H, 3.27; N, 23.15. Found: C, 55.77; H, 3.18; N, 22.97.

*3-Chloro-4-((2-oxo-2,3-dihydro-1H-benzo[d]imidazol-5-yl)amino)benzonitrile (**1e**)*

To a solution of compound **9** (179 mg, 1.2 mmol) and DIEPA (0.35 mL, 2.0 mmol) in DMSO (4 mL) was added compound **10e** (156 mg, 1.0 mmol) at rt. The mixture was stirred at 100 °C overnight and at 140 °C overnight. The reaction mixture was cooled to rt and diluted with water. The precipitated solid was collected by filtration, washed with water, and dried. The residue was suspended in EtOAc–MeOH and purified by silica gel column chromatography (EtOAc:MeOH = 10:0 to 9:1). The fractions were combined and evaporated. The residue was suspended in EtOAc, collected by filtration, washed with EtOAc, and then dried to give compound **1e** (105 mg, 0.37 mmol, 37%) as a pale purple solid. ^{1}H NMR (DMSO-d_6) 6.78–6.87 (3H, m), 6.91–6.98 (1H, m), 7.47 (1H, dd, J = 8.6, 1.9 Hz), 7.85 (1H, d, J = 2.0 Hz), 8.19 (1H, s), 10.64 (2H, s). MS *m/z* 285 $(M+H)^+$. Mp 324–326 ºC. Anal. Calcd for $C_{14}H_9ClN_4O \cdot 0.25H_2O$: C, 58.14; H, 3.31; N, 19.37. Found: C, 58.01; H, 3.18; N, 19.24.

*Methyl 3-chloro-4-((2-oxo-2,3-dihydro-1H-benzo[d]imidazol-5-yl)amino)benzoate (**1f**)*

To a solution of compound **10f** (834 mg, 4.4 mmol) and compound **9** (550 mg, 3.7 mmol) in DMSO (5 mL) was added DIPEA (1.3 mL, 7.4 mmol) at rt. The mixture was stirred at 100 °C for 1 d and heated under microwave irradiation at 160 °C for 2 h. The reaction mixture was cooled to rt, diluted with EtOAc and water, and extracted with EtOAc. The extract was washed with water and brine, dried over Na_2SO_4, and then evaporated. The residual solid was suspended in EtOAc and insoluble materials were removed by filtration. The filtrate was purified by silica

gel column chromatography (EtOAc:MeOH = 10:0 to 9:1). The fractions were combined and evaporated. The residual solid was suspended in EtOAc, collected by filtration, washed with EtOAc, and dried to give compound **1f** (17 mg, 0.05 mmol, 1%) as an off-white solid. ^{1}H NMR (DMSO-d_6) 3.78 (3H, s), 6.80–6.95 (4H, m), 7.66 (1H, dd, J = 8.7, 2.0 Hz), 7.85 (1H, d, J = 2.0 Hz), 8.03 (1H, s), 10.61 (1H, brs), 10.62 (1H, brs). MS m/z 318 $(M+H)^+$. Mp 304–306 ºC. Anal. Calcd for $C_{15}H_{12}ClN_3O_3 \cdot 0.3H_2O$: C, 55.75; H, 3.93; N, 13.00. Found: C, 55.93; H, 3.86; N, 12.75.

*3-Chloro-4-((2-oxo-2,3-dihydro-1H-benzo[d]imidazol-5-yl)amino)benzoic acid (**1g**)*

To a solution of compound **1f** (230 mg, 0.72 mmol) in MeOH (5 mL) and THF (5 mL) was added 1 M NaOH (2.9 mL, 2.9 mmol) at rt. The mixture was stirred at 50 °C for 3 h, cooled to rt, and acidified with 5% aqueous citric acid solution. The precipitated solid was collected by filtration and washed with water. The residue was dissolved in MeOH and MeCN, and evaporated. The resulting solid was suspended in MeCN–MeOH, collected by filtration, washed with MeCN, and dried to give compound **1g** (125 mg, 0.41 mmol, 57%) as a pale brown solid. ^{1}H NMR (DMSO-d_6) 6.78–6.94 (4H, m), 7.64 (1H, dd, J = 8.6, 1.9 Hz), 7.83 (1H, d, J = 2.0 Hz), 7.94 (1H, s), 10.59 (1H, brs), 10.60 (1H, brs), 12.55 (1H, brs). MS m/z 304 $(M+H)^+$. Mp 319–321 ºC. Anal. Calcd for $C_{14}H_{10}ClN_3O_3 \cdot 1.6H_2O$: C, 50.57; H, 4.00; N, 12.64. Found: C, 50.57; H, 3.86; N, 12.78.

*3-Chloro-4-((2-oxo-2,3-dihydro-1H-benzo[d]imidazol-5-yl)amino)benzamide (**1h**)*

To a solution of compound **1g** (100 mg, 0.33 mmol) and HOBt·NH_3 (65 mg, 0.43 mmol) in DMF (5 mL) was added EDC (67 mg, 0.43 mmol) at rt. The mixture was stirred at rt for 4 d, cooled to 0 °C, and diluted with water. The precipitated solid was collected by filtration, washed

with water, and dried. The resulting solid was suspended in MeOH–EtOAc, collected by filtration, washed with EtOAc, and dried to give compound **1h** (70 mg, 0.23 mmol, 70%) as a pale brown solid. ^{1}H NMR (DMSO-d_6) 6.78–6.93 (4H, m), 7.13 (1H, brs), 7.62 (1H, dd, J = 8.6, 2.0 Hz), 7.71–7.81 (2H, m), 7.89 (1H, d, J = 2.0 Hz), 10.55 (1H, s), 10.57 (1H, s). MS m/z 303 $(M+H)^+$. Mp 289–291 ºC. Anal. Calcd for $C_{14}H_{11}ClN_4O_2 \cdot 0.4H_2O$: C, 54.26; H, 3.84; N, 18.08. Found: C, 54.37; H, 3.67; N, 17.80.

*3-((4,5-Dichloro-2-nitrophenyl)amino)propan-1-ol (**13a**)*

Compound **11** (0.40 mL, 3.1 mmol) was added to a solution of DIPEA (0.80 mL, 4.6 mmol) and compound **12a** (0.23 mL, 3.1 mmol) in DMA (5 mL) at 0 °C. The mixture was stirred at rt overnight. The reaction mixture was poured into water and extracted with EtOAc. The organic layer was separated, washed with water and brine, dried over $MgSO_4$, and concentrated in vacuo. The residue was purified by silica gel column chromatography (hexane:EtOAc = 4:1 to 1:1) to give compound **13a** (723 mg, 2.73 mmol, 89 %) as an orange solid. ^{1}H NMR (DMSO-d_6) 1.70–1.80 (2H, m), 3.38–3.48 (2H, m), 3.49–3.58 (2H, m), 4.74 (1H, t, J = 5.0 Hz), 7.35 (1H, s), 8.24 (1H, s), 8.41 (1H, t, J = 5.4 Hz). MS m/z 266 $(M+H)^+$.

*5-((2-Chloro-5-((3-hydroxypropyl)amino)-4-nitrophenyl)amino)-1H-benzo[d]imidazol-2(3H)-one (**3**)*

A mixture of compound **13a** (100 mg, 0.38 mmol), compound **9** (68 mg, 0.45 mmol) and DIPEA (0.10 mL, 0.57 mmol) in DMA (1 mL) was heated at 150 °C for 30 min and then heated under microwave irradiation at 200 °C for 2 h. The mixture was poured into water and extracted with EtOAc. The organic layer was separated, washed with water and brine, dried over $MgSO_4$,

and concentrated in vacuo. The precipitate was crystallized from EtOAc to give an orange solid. The solid was purified by preparative HPLC (L-Column 2 ODS, eluted with H_2O in MeCN containing 0.1% TFA). The desired product was crystallized in the fraction, collected by filtration, and then washed with water, IPE and hexane to give compound **3** (7.2 mg, 0.019 mmol, 5 %) as an orange solid. ^{1}H NMR (DMSO-d_6) 1.48–1.75 (2H, m), 2.99–3.14 (2H, m), 3.38–3.47 (2H, m), 4.42–4.70 (1H, m), 6.03 (1H, s), 6.75–7.06 (3H, m), 8.06 (1H, s), 8.24–8.54 (2H, m), 10.22–10.96 (2H, m). MS *m/z* 378 $(M+H)^+$. Mp 294–296 ºC. Anal. Calcd for $C_{16}H_{16}ClN_5O_4 \cdot 0.1H_2O$: C, 50.63; H, 4.30; N, 18.45. Found: C, 50.61; H, 4.22; N, 18.29.

*Ethyl 3-((4,5-dichloro-2-nitrophenyl)amino)propanoate (**13b**)*

Compound **13b** was prepared from ethyl 3-aminopropanoate hydrochloride in a similar manner to that described for compound **13a** and obtained in 85% yield as an orange solid. ^{1}H NMR (DMSO-d_6) 1.18 (3H, t, *J* = 7.1 Hz), 2.67 (2H, t, *J* = 6.6 Hz), 3.59–3.68 (2H, m), 4.08 (2H, q, *J* = 7.1 Hz), 7.44 (1H, s), 8.24 (1H, s), 8.25–8.30 (1H, m). MS *m/z* 307 $(M+H)^+$.

*Ethyl 3-((4-chloro-2-nitro-5-((2-oxo-2,3-dihydro-1H-benzo[d]imidazol-5-yl)amino)phenyl)amino)propanoate (**4**)*

A mixture of compound **13b** (685 mg, 2.2 mmol), compound **9** (400 mg, 2.7 mmol) and DIPEA (0.58 mL, 3.4 mmol) in NMP (3 mL) was heated under microwave irradiation at 200 °C for 3 h. The mixture was directly charged on silica gel and purified by silica gel column chromatography (hexane:EtOAc = 3:1 to 0:10 and then EtOAc:MeOH = 10:0 to 20:1) to give a yellow solid. The solid was crystallized from EtOAc to give compound **4** (287 mg, 0.68 mmol, 31 %) as a yellow solid. ^{1}H NMR (DMSO-d_6) 1.12 (3H, t, *J* = 7.1 Hz), 2.52–2.58 (2H, m),

3.21–3.30 (2H, m), 4.01 (2H, q, *J* = 7.1 Hz), 6.04 (1H, s), 6.86–6.97 (3H, m), 8.06 (1H, s), 8.33 (1H, t, *J* = 5.2 Hz), 8.43 (1H, brs), 10.68 (2H, brs). MS *m/z* 420 $(M+H)^+$. Mp 221–223 ºC. Anal. Calcd for $C_{18}H_{18}ClN_5O_5 \cdot H_2O$: C, 49.38; H, 4.60; N, 16.00. Found: C, 49.12; H, 4.48; N, 15.86.

*3-((4-Chloro-2-nitro-5-((2-oxo-2,3-dihydro-1H-benzo[d]imidazol-5-yl)amino)phenyl)amino)propanoic acid (**5**)*

A mixture of compound **4** (50 mg, 0.12 mmol) and 2 M NaOH in H_2O (1 mL, 2.0 mmol) in THF (1 mL) and MeOH (1 mL) was stirred at rt overnight. The mixture was neutralized with 1 M HCl at 0 °C and extracted with EtOAc. The organic layer was washed with water and brine, dried over $MgSO_4$, and concentrated in vacuo. The residue was crystallized from EtOAc–hexane to give compound **5** (22 mg, 0.056 mmol, 47 %) as a yellow solid. ^{1}H NMR (DMSO-d_6) 2.39–2.48 (2H, m), 3.16–3.28 (2H, m), 6.08 (1H, s), 6.88–6.97 (3H, m), 8.06 (1H, s), 8.33 (1H, t, *J* = 5.2 Hz), 8.42 (1H, s), 10.67 (2H, d, *J* = 3.6 Hz), 12.40 (1H, brs). MS *m/z* 392 $(M+H)^+$. Mp 282–284 ºC. Anal. Calcd for $C_{16}H_{14}ClN_5O_5 \cdot 0.1EtOAc \cdot 0.3H_2O$: C, 48.52; H, 3.82; N, 17.25. Found: C, 48.69; H, 3.70; N, 17.01.

*4,5-Dichloro-2-nitro-N-(pyridin-3-ylmethyl)aniline (**13c**)*

A mixture of compound **11** (2.5 g, 12 mmol), compound **12c** (1.3 g, 12 mmol) and TEA (1.7 mL, 12 mmol) in DMSO (30 mL) was stirred at rt for 3 h. The mixture was diluted with EtOAc, washed with water and brine, dried over Na_2SO_4 and concentrated in vacuo. The residue was washed with IPE to give compound **13c** (3.0 g, 10 mmol, 85 %) as a yellow solid. ^{1}H NMR ($CDCl_3$) 4.55 (2H, d, *J* = 5.7 Hz), 6.93 (1H, s), 7.34 (1H, dd, *J* = 7.7, 4.7 Hz), 7.62–7.70 (1H, m), 8.23–8.36 (2H, m), 8.56–8.69 (2H, m). MS *m/z* 298 $(M+H)^+$.

*5-((2-Chloro-4-nitro-5-((pyridin-3-ylmethyl)amino)phenyl)amino)-1H-benzo[d]imidazol-2(3H)-one (**6**)*

$Pd_2(dba)_3$ (31 mg, 0.030 mmol) was added to a solution of compound **13c** (200 mg, 0.67 mmol), compound **9** (100 mg, 0.67 mmol), cesium carbonate (328 mg, 1.0 mmol) and BINAP (42 mg, 0.070 mmol) in DME (5 mL). The mixture was stirred at 100 °C under N_2 for 4 h and then diluted with EtOAc and water. The precipitate was collected by filtration. The solid was purified by preparative HPLC (L-Column 2 ODS, eluted with H_2O in MeCN containing 0.1% TFA). To the desired fraction was added aqueous $NaHCO_3$ solution and concentrated into half volume in vacuo. The precipitate was collected by filtration to give compound **6** (15 mg, 0.037 mmol, 5 %) as a light brown solid. ^{1}H NMR (DMSO-d_6) 4.37 (2H, d, J = 5.7 Hz), 5.87 (1H, s), 6.42 (1H, d, J = 8.2 Hz), 6.68 (1H, s), 6.80 (1H, d, J = 8.2 Hz), 7.22–7.27 (1H, m), 7.46 (1H, d, J = 7.6 Hz), 8.06 (1H, s), 8.30 (2H, brs), 8.45 (1H, d, J = 4.4 Hz), 8.85 (1H, t, J = 6.0 Hz), 10.65 (2H, d, J = 12.7 Hz). MS m/z 411 $(M+H)^+$. Mp 298–300 ºC. Anal. Calcd for $C_{19}H_{15}ClN_6O_3 \cdot 0.1H_2O$: C, 55.31; H, 3.71; N, 20.37. Found: C, 55.22; H, 3.59; N, 20.24.

*N-(4,5-Dichloro-2-nitrophenyl)tetrahydro-2H-pyran-4-amine (**13d**)*

Compound **11** (0.40 mL, 3.1 mmol) was added to a solution of DIPEA (0.80 mL, 4.6 mmol) and compound **12d** (310 mg, 3.1 mmol) in DMSO (5 mL) at rt. The mixture was stirred at rt overnight. The mixture was poured into water and extracted with EtOAc. The organic layer was separated, washed with aqueous citric acid solution and brine, dried over $MgSO_4$, and concentrated in vacuo. The residue was purified by silica gel column chromatography (hexane:EtOAc = 3:1 to 3:2) to give compound **13d** (784 mg, 2.7 mmol, 88 %) as an orange

solid. ^{1}H NMR ($CDCl_3$) 1.59–1.78 (2H, m), 2.01–2.11 (2H, m), 3.53–3.73 (3H, m), 4.03 (2H, dt, *J* = 12.0, 3.8 Hz), 6.98 (1H, s), 8.01 (1H, d, *J* = 6.5 Hz), 8.30 (1H, s). MS *m/z* 291 $(M+H)^+$.

*5-((2-Chloro-4-nitro-5-((tetrahydro-2H-pyran-4-yl)amino)phenyl)amino)-1H-benzo[d]imidazol-2(3H)-one (**7**)*

A mixture of compound **13d** (300 mg, 1.0 mmol), compound **9** (184 mg, 1.2 mmol) and DIPEA (0.22 mL, 1.2 mmol) in NMP (1 mL) was heated under microwave irradiation at 200 °C for 3 h. The mixture was directly charged on silica gel and purified by silica gel column chromatography (hexane:EtOAc = 3:1 to 0:10 and then EtOAc:MeOH = 10:0 to 9:1) and following preparative HPLC (L-Column 2 ODS, eluted with H_2O in MeCN containing 0.1% TFA). The desired fraction was concentrated in vacuo. The residue was washed with water, IPE and hexane to give compound **7** (55 mg, 0.14 mmol, 13 %) as an orange solid. ^{1}H NMR (DMSO-d_6) 1.40–1.55 (2H, m), 1.74–1.87 (2H, m), 3.19–3.30 (3H, m), 3.74–3.84 (2H, m), 6.12 (1H, s), 6.87–6.98 (3H, m), 8.07 (1H, s), 8.12 (1H, d, *J* = 7.0 Hz), 8.48 (1H, brs), 10.69 (2H, brs). MS *m/z* 404 $(M+H)^+$. Mp 305–307 ºC. Anal. Calcd for $C_{18}H_{18}ClN_5O_4 \cdot 0.25H_2O$: C, 52.95; H, 4.57; N, 17.15. Found: C, 53.07; H, 4.37; N, 16.98.

*4-(4,5-Dichloro-2-nitrophenoxy)tetrahydro-2H-pyran (**13e**)*

Compound **12e** (1.5 mL, 15 mmol) was added to a suspension of sodium hydride (60% wt, 0.67 g, 17 mmol) in DMF (30 mL) at 0 °C. After being stirred at 0 °C for 20 min, compound **11** (2.0 mL, 15 mmol) was added to the reaction mixture. The mixture was stirred at rt for 20 min. The mixture was quenched with water at rt and extracted with EtOAc. The organic layer was separated, washed with water and brine, dried over $MgSO_4$, and concentrated in vacuo. The

residue was purified by silica gel column chromatography (hexane:EtOAc = 10:0 to 3:1) to give compound **13e** (2.6 g, 8.9 mmol, 58 %) as a pale yellow solid. ^{1}H NMR ($CDCl_3$) 1.78–1.96 (2H, m), 1.97–2.16 (2H, m), 3.51–3.75 (2H, m), 3.89–4.06 (2H, m), 4.46–4.80 (1H, m), 7.18 (1H, s), 7.98 (1H, s).

*5-((2-Chloro-4-nitro-5-((tetrahydro-2H-pyran-4-yl)oxy)phenyl)amino)-1H-benzo[d]imidazol-2(3H)-one (**8a**)*

Compound **8a** was prepared from compound **13e** in a similar manner to that described for compound **6** and obtained in 47% yield as a yellow solid. ^{1}H NMR (DMSO-d_6) 1.52–1.65 (2H, m), 1.78–1.91 (2H, m), 3.37–3.51 (2H, m), 3.70–3.82 (2H, m), 4.41–4.50 (1H, m), 6.51 (1H, s), 6.85–6.97 (3H, m), 8.07 (1H, s), 8.45 (1H, s), 10.66 (1H, s), 10.69 (1H, s). MS *m*/*z* 405 $(M+H)^+$. Mp 309–311 ºC. Anal. Calcd for $C_{18}H_{17}ClN_4O_5 \cdot 0.25H_2O$: C, 52.82; H, 4.31; N, 13.69. Found: C, 53.00; H, 4.33; N, 13.46.

*5-((2-Chloro-4-nitro-5-((tetrahydro-2H-pyran-4-yl)oxy)phenyl)amino)indolin-2-one (**8b**)*

Compound **8b** was prepared from compound **13e** and 5-aminoindolin-2-one in a similar manner to that described for compound **6** and obtained in 17% yield as a yellow solid. ^{1}H NMR (DMSO-d_6) 1.53–1.65 (2H, m), 1.80–1.91 (2H, m), 3.40–3.53 (4H, m), 3.70–3.82 (2H, m), 4.44–4.53 (1H, m), 6.46 (1H, s), 6.85 (1H, d, *J* = 8.1 Hz), 7.09–7.19 (2H, m), 8.07 (1H, s), 8.45 (1H, s), 10.43 (1H, s). MS *m*/*z* 404 $(M+H)^+$. Mp 222–224 ºC. Anal. Calcd for $C_{19}H_{18}ClN_3O_5 \cdot 0.25H_2O$: C, 55.89; H, 4.57; N, 10.29. Found: C, 55.87; H, 4.59; N, 10.19.

*6-((2-Chloro-4-nitro-5-((tetrahydro-2H-pyran-4-yl)oxy)phenyl)amino)-3,4-dihydroquinolin-2(1H)-one (**8c**)*

Compound **8c** was prepared from compound **13e** and 6-amino-3,4-dihydroquinolin-2(1*H*)-one in a similar manner to that described for compound **6** and obtained in 56% yield as a yellow solid. ^{1}H NMR (DMSO-d_6) **1.55**–1.68 (2H, m), 1.82–1.93 (2H, m), 2.43–2.52 (2H, m), 2.87 (2H, t, *J* = 7.5 Hz), 3.39–3.50 (2H, m), 3.72–3.83 (2H, m), 4.47–4.56 (1H, m), 6.55 (1H, s), 6.88 (1H, d, *J* = 8.3 Hz), 7.08–7.18 (2H, m), 8.07 (1H, s), 8.45 (1H, s), 10.14 (1H, s). Mp 222–224 ºC. Anal. Calcd for $C_{20}H_{20}ClN_3O_5 \cdot 0.1H_2O$: C, 57.24; H, 4.85; N, 10.01. Found: C, 57.22; H, 4.78; N, 9.97.

5.2. Biology

5.2.1. Cell-free ELISA

The biotinylation to -amino group of Lys in the C-terminus of Lys on the BCoR peptide was carried out with Biotin-(AC5)2 Sulfo-OSu (341-06801, Dojindo) according to the protocol recommended by the manufacturer. The wells of a Nunc Maxisorp microplate (460-518) were coated with streptavidin (SA) (191-12851, Wako) and were blocked with PBS that contained 1.0% casein. Biotinylated BCoR peptide was captured by the SA, and wt BCL6^{BTB} (0.5 nM) solution with PBS containing 0.05 % Tween20 and 1 mM DTT (PBST) was added to the wells. After washing with PBST, bound BCL6^{BTB} was detected using horseradish peroxidase (HRP)-conjugated anti-FLAG antibody (A8592-1MG, Sigma). The amount of HRP in the wells was measured by using a luminescent reagent (37069, Thermo Fisher Scientific Inc.).[21] Percent inhibition was calculated based on wells without BCL6^{BTB} as high controls and without compound as low controls.

5.2.2. SPR assay

SPR biosensing experiments were performed at 22 °C on a Biacore 4000 instrument equipped with SeriesS CM5 sensor chips (GE Healthcare).

HBS-P+ (10 mM Hepes, pH 7.4, 150 mM NaCl, 0.05 % Surfactant P20, GE Healthcare) supplemented with 1 mM DTT was used as the running buffer for immobilization. NeutrAvidin (Thermo Fisher) was covalently coupled onto the sensor chip following the standard amine coupling procedure according to the manufacturer's instructions. Typical immobilization levels of NeutrAvidin ranged from 10,000 to 13,000 resonance units (RUs). Subsequently avi-tagged wt $BCL6^{BTB}$ was injected onto the NeutrAvidin-immobilized sensor chip. The surfaces were blocked by injecting biocytin (Thermo Fisher). Approximately 13,000 RUs of wt $BCL6^{BTB}$ were captured by NeutrAvidin.

For the interaction studies, binding experiments were performed in 20 mM Tris, pH 8.0, 150 mM NaCl, 0.01% Surfactant P20, 1 mM DTT, and 5% DMSO. Sample solutions of different concentrations were injected for 30 or 90 s at a flow rate of 30 µL/min and the dissociation followed thereafter for up to 30 or 240 s. Data processing and analysis were performed using the Biacore 4000 evaluation software (GE Healthcare). Solvent correction was included as described in the Biacore software handbook. Sensorgrams were double-referenced prior to fitting the concentration series to a steady-state affinity model. The dissociation constant K_D was calculated using the equation below.

$$K_D = R_{max} \times C/R\text{-}C$$

where R_{max}, R, and C correspond to the sample binding capacity of the surface (RU), the normalized response of the test sample (RU), and the concentration of the test solution (M), respectively.

5.2.3. M2H assay

The assay was performed according to a procedure described previously.[5] The vectors pGL4.35, pBind, and pACT were obtained from Promega Corp. As template DNA, human BCL6 cDNA was isolated by PCR from a human skeletal muscle cDNA library (Takara Bio) and human BCoR cDNA was purchased from GeneCopoeia Inc. Each cDNA fragment was granted a restriction site by PCR and was digested with restriction enzymes to insert into pBIND or pACT, respectively. M2H was performed in HEK293T cells that were transfected with reporter constructs: pGL4.35 containing GAL4 special response element of firefly luciferase (9×GAL4UAS), pBIND/GAL4-BCL6 (Ala5–Glu129), and pACT/VP16-BCOR (Leu112–Ala753) by Fugene HD (Promega). The transfected cells were seeded at 1×10^4 cells/15 μL/well on 384-well plates (3570, Corning) in Dulbecco's Modified Eagle's Medium (DMEM) containing 10% FBS. After incubation for 2 h, 15 μL of compounds at various concentrations in DMEM that contained 10% FBS were added to the wells and incubated for a further 20 hours at 37 °C under 5% CO_2. Cells were lysed to measure luciferase activity using the Bright-Glo luciferase assay system (Promega).[21] Percent inhibition was calculated based on wells without transfection of pBIND/GAL-BCL6 (Ala5–Glu129) as high controls and wells without compound as low controls.

5.2.4. Aqueous solubility

Small volumes of the compound solution dissolved in DMSO were added to the aqueous buffer solution (pH 6.8). After incubation, precipitates were separated by filtration. The solubility was determined by UV absorbance of each filtrate.

5.2.5. PAMPA

The donor wells were filled with 200 μL of PRISMA HT buffer (pH 7.4, Pion Inc.) containing 10 μmol/L test compound. The filter on the bottom of each acceptor well was coated with 4 μL of GIT-0 Lipid Solution (Pion Inc.) and filled with 200 μL of Acceptor Sink Buffer (Pion Inc.). The acceptor filter plate was put on the donor plate and incubated for 3 h at rt. After incubation, the amount of test compound in both the donor and acceptor wells was measured by LC/MS/MS.

5.2.6. Cytotoxicity assay

HepG2 cells were seeded at 5×10^3 cells/well in 384-well white plates, and cultured in DMEM supplemented with 0.5% fetal bovine serum and test compound for 24 hours. The cell viability was determined based on the cellular ATP content. The cellular ATP content was measured by CellTiter-Glo reagent (Promega) according to the manufacturer's instructions. ATP content was calculated using the following formula:

ATP content (% of control) = (RLU of test compound / RLU of 1% DMSO) × 100.

5.2.7. X-ray crystallography

Crystals of unliganded FLAG-BCL6^{BTB} (5–129) for soaking experiments were obtained as described previously.[21] Crystallization was performed by vapor diffusion using the sitting-drop method using 0.1 M Bis-Tris at pH 6.5, 0.7 M potassium/sodium tartrate at 20 °C. To generate protein-ligand complexes, crystals were typically soaked for 2 h in a reservoir solution containing 1 mM ligand. Prior to data collection, crystals were immersed in the reservoir solution with the addition of 30% glycerol as a cryoprotectant and were flash-frozen in liquid nitrogen. Diffraction data were collected from a single crystal using the CCD detector Quantum 315 (ADSC) at beamline 5.0.2 of Advanced Light Source (CA, USA) and the CCD detector Quantum 270 (ADSC) at beamline AR-NE3A of Photon Factory (Tsukuba, Japan) under a 100 K nitrogen cryostream. The data were reduced and scaled with HKL2000.[27] The structure was solved by the molecular replacement method with Molrep[28] of the CCP4 program suites[29] using the BCL6^{BTB} structure (PDB code: 1R28) as a search model. The structure was refined through an iterative procedure utilizing REFMAC[30] followed by model building in COOT.[31] The final models were validated using Molprobity.[32] Crystallographic processing and refinement statistics are summarized in Supporting Information Table S1. All structural figures were generated using PyMOL (Schrödinger). Atom coordinates and structure factors have been deposited in the Protein Data Bank with accession codes: 5X9O (BCL6/**1a**) and 5X9P (BCL6/**5**), and will be released upon article publication.

Acknowledgments

The authors would like to thank Takayuki Tatamiya, Hideyuki Oki, Tomoya Sameshima, Ikuo Miyahisa, Misaki Homma, Michiyo Mochizuki, Takashi Ichikawa, and Nobuo Cho for their kind

suggestions. We gratefully acknowledge Takamichi Muraki, Katsunori Sasa, and Shigeru Kondo for their kind support of compound evaluation. We are grateful to Ikumi Chisaki and Shin-ichi Niwa for describing a part of the experimental section. We also thank the staff of the Berkeley Center for Structural Biology who operate the beamlines 5.0.2 of Advanced Light Source (CA, USA). Berkeley Center for Structural Biology is supported in part by the U.S. National Institutes of Health and U.S. National Institute of General Medical Sciences. The Advanced Light Source is supported by the Director, Office of Science, Office of Basic Energy Sciences of the U.S. Department of Energy under Contract No. DE-AC02-05CH11231. We also thank the staff of the Structural Biology Research Center who operate the PF beamlines.

Supplementary data.

Supplementary data associated with this article can be found, in the online version, at http...

References and notes

1. Parekh S, Polo JM, Shaknovich R, Juszczynski P, Lev P, Ranuncolo SM, Yin Y, Klein U, Cattoretti G, Favera RD, Shipp MA, Melnick A. BCL6 programs lymphoma cells for survival and differentiation through distinct biochemical mechanisms. *Blood* 2007;110:2067–2074.

2. Melnick A, Carlile G, Ahmad KF, Kiang C-L, Corcoran C, Bardwell V, Prive GG, Licht JD. Critical residues within the BTB domain of PLZF and Bcl-6 modulate interaction with corepressors. *Mol. Cell. Biol*. 2002;22:1804–1818.

3. Ghetu AF, Corcoran CM, Cerchietti L, Bardwell VJ, Melnick A, Prive GG. Structure of a BCOR corepressor peptide in complex with the BCL6 BTB domain dimer. *Mol. Cell* 2008;29:384–391.

4. Ahmad K. F, Melnick A, Lax S, Bouchard D, Liu J, Kiang CL, Mayer S, Takahashi S, Licht JD, Prive GG. Mechanism of SMRT corepressor recruitment by the BCL6 BTB domain. *Mol. cell* 2003;12:1551-1564.

5. Huynh KD, Bardwell VJ. The BCL-6 POZ domain and other POZ domains interact with the co-repressors N-CoR and SMRT. *Oncogene* 1998;17:2473-2484.

6. Cattoretti G, Chang CC, Cechova K, Zhang J, Ye BH, Falini B, Louie DC, Offit K, Chaganti RS, Dalla-Favera R. BCL-6 protein is expressed in germinal-center B cells. *Blood* 1995;86:45-53.

7. Huynh KD, Fischle W, Verdin E, Bardwell VJ. BCoR, a novel corepressor involved in BCL-6 repression. *Genes Dev*. 2000;14:1810-1823.

8. Xin N, Fu L, Shao Z, Guo M, Zhang X, Zhang Y, Dou C, Zheng S, Shen X, Yao Y, Wang J, Wang J, Cui G, Liu Y, Geng D, Xiao C, Zhang Z, Dong R. RNA interference targeting Bcl-6 ameliorates experimental autoimmune myasthenia gravis in mice. *Mol. Cell. Neurosci*. 2014;58:85-94.

9. Dent AL, Shaffer AL, Yu X, Allman D, Staudt LM. Control of inflammation, cytokine expression, and germinal center formation by BCL-6. *Science* 1997;276:589-592.

10. Linterman MA, Vinuesa CG. Signals that influence T follicular helper cell differentiation and function. *Semin. Immunopathol*. 2010;32:183-196.

11. Basso K, Dalla-Favera R. Roles of BCL6 in normal and transformed germinal center B cells. *Immunological Reviews* 2012;247:172–183.

12. Duy C, Hurtz C, Shojaee S, Cerchietti L, Geng H, Swaminathan S, Klemm L, Kweon SM, Nahar R, Braig M, Park E, Kim YM, Hofmann WK, Herzog S, Jumaa H, Koeffler HP, Yu JJ, Heisterkamp N, Graeber TG, Wu H, Ye BH, Melnick A, Muschen M. BCL6 enables Ph+ acute lymphoblastic leukaemia cells to survive BCR-ABL1 kinase inhibition. *Nature* 2011;473:384-388.

13. Parekh S, Prive G, Melnick A. Therapeutic targeting of the BCL6 oncogene for diffuse large B-cell lymphomas. *Leuk. Lymphoma* 2008;49:874-882.

14. Cerchietti LC, Yang SN, Shaknovich R, Hatzi K, Polo JM, Chadburn A, Dowdy SF, Melnick A. A peptomimetic inhibitor of BCL6 with potent antilymphoma effects *in vitro* and *in vivo*. *Blood* 2009;113:3397–3405.

15. Evans SE, Goult BT, Fairall L, Jamieson AG, Ferrigno PK, Ford R, Schwabe JWR, Wagner SD. The Ansamycin Antibiotic, Rifamycin SV, Inhibits BCL6 Transcriptional Repression and Forms a Complex with the BCL6-BTB/POZ Domain. *Plos One* 2014;9:e90889.

16. Cerchietti LC, Ghetu AF, Zhu X, Da Silva GF, Zhong S, Matthews M, Bunting KL, Polo JM, Fares C, Arrowsmith CH, Yang SN, Garcia M, Coop A, MacKerell Jr. AD, Prive GG, Melnick A. A small-molecule inhibitor of BCL6 kills DLBCL cells *in vitro* and *in vivo*. *Cancer Cell* 2010;17:400–411.

17. Cardenas MG, Yu W, Beguelin W, Teater MR, Geng H, Goldstein RL, Oswald E, Hatzi K, Yang S-N, Cohen J, Shaknovich R, Vanommeslaeghe K, Cheng H, Liang D, Cho HJ, Abbott J, Tam W, Du W, Leonard JP, Elemento O, Cerchietti L, Cierpicki T, Xue F, MacKerell Jr.

AD, Melnick A. Rationally designed BCL6 inhibitors target activated B cell diffuse large B cell lymphoma. *J. Clin. Invest*. 2016;126:3351–3362.

18. Arkin MR, Wells JA. Small-molecule inhibitors of protein-protein interactions: progressing towards the dream. *Nature Rev*. 2004;3:301–317.

19. Fuller JC, Burgoyne NJ, Jackson RM. Predicting druggable binding sites at the protein–protein interface. *Drug Discov. Today* 2009;14:155–161.

20. Wells JA, McClendon CL. Reaching for high-hanging fruit in drug discovery at protein–protein interfaces. *Nature* 2007;450:1001–1009.

21. Sakamoto K, Sogabe S Kamada Y, Sakai N, Asano K, Yoshimatsu M, Ida K, Imaeda Y, Sakamoto J. Discovery of high-affinity BCL6-binding peptide and its structureactivity relationship. *Biochem. and Biophys. Res. Commun*. 2017;482:310–316.

22. After preparation of this manuscript, following two papers on discovery of BCL6 inhibitors by fragment-based approaches were reported from our group and McCoull *et al*.; (a) Kamada Y, Sakai N, Sogabe S, Ida K, Oki H, Sakamoto K, Lane W, Snell G, Iida M, Imaeda Y, Sakamoto J, Matsui J. Discovery of a B‑Cell Lymphoma 6 Protein–Protein Interaction Inhibitor by a Biophysics-Driven Fragment-Based Approach. *J. Med. Chem.* 2017;60:4358–4368; (b) McCoull W, Abrams RD, Anderson E, Blades K, Barton P, Box M, Burgess J, Byth K, Cao Q, Chuaqui C, Carbajo RJ, Cheung T, Code E, Ferguson AD, Fillery S, Fuller NO, Gangl E, Gao N, Gris, M, Hargreaves D, Howard MR, Hu J, Kemmitt PD, Nelson JE, O'Connell N, Prince DB, Raubo P, Rawlins PB, Robb GR, Shi J, Waring MJ, Whittaker D, Wylot M, Zhu X. Discovery of Pyrazolo[1,5‑a]pyrimidine B‑Cell Lymphoma

6 (BCL6) Binders and Optimization to High Affinity Macrocyclic Inhibitors. *J. Med. Chem.* 2017;60:4386–4402.

23. In order to perform the docking simulation, the X-ray structure of **1a** with $BCL6^{BTB}$ was used as a template. The docking site was manually selected with reference to the binding site of **1a** after determination of a ligand-binding site by site finder of MOE (version 2015.10, Chemical Computing Group Inc., Montreal, Canada) under default settings. After docking calculation by using the standard docking methods implemented in MOE, complex structure of docked compounds with $BCL6^{BTB}$ was energy-minimized using the Amber10:EHT force field in MOE to obtain the final docking model. During the minimization procedure, the standard default settings were used except that whole $BCL6^{BTB}$ structure was fixed completely.

24. Yokoyama T, Taft WR, Kamlet M. The solvatochromic comparison method. 3. Hydrogen bonding by some 2-nitroaniline derivatives. *J. Am. Chem. Soc*. 1976;98:3233–3237.

25. Ishikawa M, Hashimoto Y. Improvement in aqueous solubility in small molecule drug discovery programs by disruption of molecular planarity and symmetry. *J. Med. Chem.* 2011;54:1539–1554.

26. Buchwald P. Small-molecule protein–protein interaction inhibitors: therapeutic potential in light of molecular size, chemical space, and ligand binding efficiency considerations. *IUBMB Life* 2010;62:724–731.

27. Otwinowski Z, Minor W. Processing of X-ray diffraction data collected in oscillation mode. In *Macromolecular Crystallography, part A*, Carter CWJ, Sweet RM. Eds. Academic Press: New York 1997;276:307–326.

28. Vagin A, Teplyakov A. MOLREP: an Automated Program for Molecular Replacement. *J. Appl. Cryst*. 1997;30:1022–1025.

29. Collaborative Computational Project, N. The CCP4 suite: programs for protein crystallography. *Acta Crystallogr. D, Biol. Crystallogr*. 1994;50:760–763.

30. Murshudov GN, Skubak P, Lebedev AA, Pannu NS, Steiner RA, Nicholls RA, Winn MD, Long F, Vagin AA. REFMAC5 for the refinement of macromolecular crystal structures. *Acta Crystallogr. D, Biol. Crystallogr*. 2011;67:355–367.

31. Emsley P, Lohkamp B, Scott WG, Cowtan K. Features and development of Coot. *Acta Crystallogr. D, Biol. Crystallogr*. 2010;66:486–501.

32. Chen VB, Arendall WB. 3rd, Headd JJ, Keedy DA, Immormino RM, Kapral GJ, Murray LW, Richardson JS, Richardson DC. MolProbity: all-atom structure validation for macromolecular crystallography. *Acta Crystallogr. D, Biol. Crystallogr*. 2010;66:12–21.